

Characterization of Ti-containing amorphous carbon films prepared on titanium substrates

D. SHEEJA*, B. K. TAY*, C. Q. SUN*, Y. Q. FU†

*School of Electrical and Electronic Engineering, †School of Mechanical and Production Engineering, Nanyang Technological University, Singapore 639798, Republic of Singapore
E-mail: esheeja@ntu.edu.sg

Amorphous carbon (a:C) films prepared on pure titanium (Ti) substrates exhibit relatively high intrinsic compressive stress. In order to obtain low stress films with varied electrical and mechanical properties, metal (Ti) ions are incorporated into the plasma. This is done with the help of metal containing carbon targets. Amorphous carbon films with varied percentage of Ti were deposited on polished pure Ti substrates using Filtered Cathodic Vacuum Arc (FCVA) technique together with substrate pulse biasing. Characterizations of the films were carried out using various equipments including Raman Spectroscopy, X-ray diffractometer, Atomic Force Microscopy (AFM), Pin-on-Disk Tribometer and Micro-Scratch Tester; and properties such as microstructure, crystallography, film stress, morphology, frictional coefficient and critical load were investigated as a function of Ti content in the target. The results suggest that the film prepared with 5 at.% Ti-containing carbon target, under 7 kV substrate pulse bias voltage, displays almost zero stress. However such films are inferior in its Tribological properties compared to that of pure a:C films.

© 2003 Kluwer Academic Publishers

1. Introduction

The tetrahedral amorphous carbon (ta:C) films with high sp^3 content have proven to be a viable alternative to diamond in a number of applications. A wide variety of deposition methods have been used to prepare diamond-like carbon films. The recent research shows that the ta:C films produced by Filtered Cathodic Vacuum Arc Technique exhibit relatively good qualities compared to that by other techniques [1–5]. However, it is recognized that a high level of intrinsic compressive stress in these films has severely restricted the practical applications of these materials. Therefore, investigations are being carried out to find ways to reduce the stress in these films. Much of the researches concentrated in this area are by annealing [6–8], incorporating a small percentage of metal ions in the films [9, 10] and preparations of the films under substrate pulse biasing [4, 11]. It has been found that the stress in pure a:C films prepared on Ti metal substrates is relatively high [12]. The low stress, metal incorporated a:C films can have a wider range of applications, for e.g., thin film passive devices such as resistors. In this paper, we study the effect of different percentage of Ti-containing a:C (Ti-a:C) films prepared under the same conditions. Characterisations of the films were carried out to examine the properties of the films.

2. Experimental details

2.1. Sample preparation

Pure Ti substrates of 30 mm diameter and 3 mm thickness were ground and polished to get mirror like

smoothness. The grinding and polishing was done in many stages. The first stage of grinding was done with 240 grit silicon carbide abrasive papers, followed by 400, 800 and 1200 grit abrasive papers. Subsequently the ground surfaces were polished with coarse and fine alumina solution to get mirror-like smoothness. The polished substrates were cleaned with soap solution, followed by water, acetone, isopropyl alcohol and DI water in an ultrasonic bath tank and dried with a nitrogen blow off gun. The samples were then analysed for its roughness values using a TENCOR P-10 Surface Profiler, and the average surface roughness values of the samples were maintained at around $0.1 \mu\text{m}$.

The cleaned samples were then fixed onto a sample holder, which is designed especially for the high voltage substrate bias, and is placed in the deposition chamber of the FCVA system. The schematic diagram of the FCVA deposition system is shown in Fig. 1. The whole system includes a cathodic arc source, plasma filtering duct and a deposition chamber. The cathodic arc source consists of five parts: power supply, arc striker, target material (cathode), water-cooled target holder and magnetic coil for controlling the motion of the cathode spots. The anode is connected to the ground (deposition chamber) and the cathode is connected to the target source. The arc striker is also connected to the ground to initiate an arc. The arc can be ignited by bringing the striker to the cathode surface and quickly breaking the circuit. Afterwards the arc can sustain by itself for few minutes. The plasma is then pass through an Off-Plane-Double-Bend (OPDB) filter that consists of a toroidal

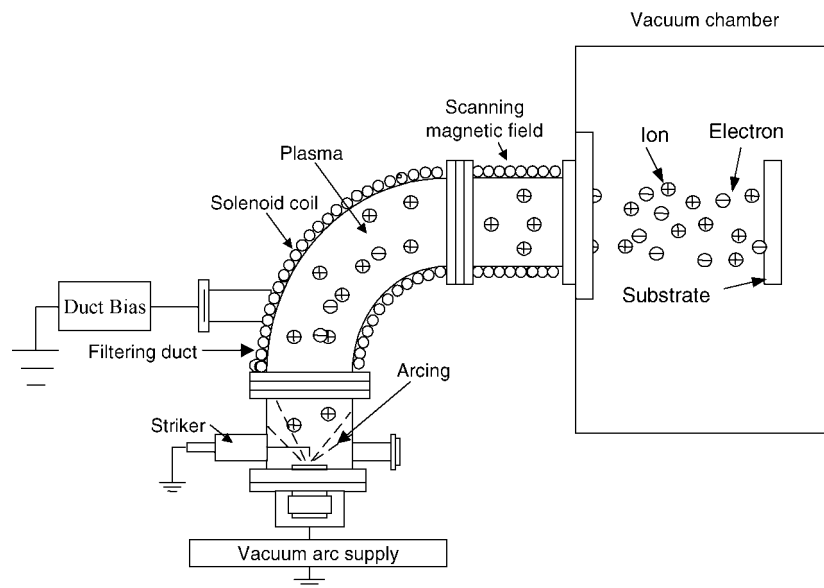


Figure 1 Schematic diagram of the FCVA deposition system.

solenoid, which is a conductive stainless torus with the copper coil wound outside. The torus allows no line-of-sight path between the cathodic arc source and the substrate, thus preventing neutral particles from reaching the substrate, while the plasma will be confined and guided by the curvilinear magnetic field of the toroidal solenoid. The deposition chamber is placed at the exit of the filter. In between there is a straight section wound with copper coil producing magnetic field to focus the plasma flux.

More details of the FCVA system is described in detail elsewhere [13]. Prior to deposition, Ar ions were used to sputter clean the oxide layer on the substrate surface for 20 minutes. A pure graphite target, 1, 5, 10 and 20 percentages of Ti-containing carbon targets were used in the study. Pure elementary powders of graphite (99.5% purity, 325 mesh) and Ti (99.5% purity, 560 mesh) were mixed thoroughly and then compacted into cylindrical targets of 60 mm diameter. The base chamber pressure was below 5×10^{-6} Torr. However, the pressure increased to 5×10^{-5} Torr during deposition. The substrate pulse biasing parameters were set at 7 kV bias voltage at a frequency of 300 Hz with a pulse width of 25 μ s, which is equivalent to a duty cycle (pulse on-time) of 0.75% (Note: a very short pulse on-time can reduce the stress in the film significantly and is reported elsewhere [11]; the probable reason could be the bombardment of highly energised (~ 7000 eV) ion and the subsequent re-arrangement of the atoms during the growth). The arc current was set to 75 A. Most of the macro-particles and neutrals were eliminated through the curved-toroidal duct. All the films were deposited at room temperature and the deposition time was varied from 10–20 min to produce a film of about 150 nm thick. It is observed that the deposition rate decreases slightly with increasing metal content in the target.

2.2. Characterisation

The micro-structural behaviour of the films was studied by using a Renishaw Raman spectroscopy using 514.5 nm lines of argon laser as the excitation source.

The Raman spectra were acquired over the range of 1–2000 cm^{-1} . The spectra were then fitted with two Gaussian peaks, using a least-square computer program called PeakFit. The peak that is centred at around 1360 cm^{-1} (disorder peak “D”) is due to small-sized graphite regions and other peak centred at around 1590 cm^{-1} (graphite peak “G”), is due to the in plane Raman mode of graphite. The parameters such as relative intensity ratio of the “D” and “G” peaks (I_D/I_G), G-peak width etc., are used to evaluate the characteristics of the film [14–18].

The nano-crystalline-structure of the Ti-a:C films were characterised by a X-ray diffractometer (XRD). The experiments were performed on a Siemens D5005 machine with a glancing incident mode by using $\text{CuK}\alpha$ radiation (50 kV, 20 mA). Since the film is thin, the incident angle was set at a low value of 0.5° . The 2θ scanning step sizes were set as 0.05° and the counting time at each step was 4.0 s. The scan range was from 30 to 80° and rotation speed is set at 50 rpm. The estimates of residual stress in the films were also determined using XRD. The roughness of the Ti-a:C films were measured from their surface morphology, which is obtained from an Atomic Force Microscopy (AFM) in tapping mode (Digital Instruments, 5-3000).

The Tribological characterisations of the films were carried out on a ball-on-disk tribometer, supplied by CSEM instruments. The tests were carried out with an applied load of 2 N and a sliding speed of 3 cm/s, with sapphire ball (6 mm diameter) counter-face. The humidity level was between 60% and 70%, while the temperature was about 23°C . The scratch tests were performed using the CSEM Micro Scratch Tester to get a semi-quantitative evaluation of the adhesion of the films. A scratch length of 6 mm and a progressive normal load of 0–5 N was set for all the tests. The loading rate and scratching speed were set at 5 N/min and 6 mm/min respectively. Determination of the Critical loads (the load at which the film peels off from the substrate) was based on acoustic emission, tangential frictional force and optical observation.

3. Experimental results

3.1. Raman spectra

Fig. 2 shows the Raman Spectra of the Ti-a:C films that contain different atomic percentage of Ti. The spectra exhibit a broad Raman intensity peak in the range of 1100–1700 cm^{-1} centred at around 1550 cm^{-1} , which is due to the sp^2 -bonded carbon structures [14, 18]. It is also obvious from the Figure that the absolute intensity of the amorphous carbon peak ($\sim 1550 \text{ cm}^{-1}$) decreases with the increase of Ti content in the films. This could be due to the lowering of the pure graphite clusters in the film. The actual Ti content in the film could be as high as two times that of the corresponding target [19]. The 20 at.% Ti-a:C film exhibits an extremely weak carbon peak and this could be due to the fact that, major fraction of the carbon atoms in the film exist in the form of titanium carbide (see XRD patterns).

In order to analyse the Raman spectra quantitatively, the broad peak around 1550 cm^{-1} is deconvoluted to “D” and “G” peaks. The intensity ratio of the peaks

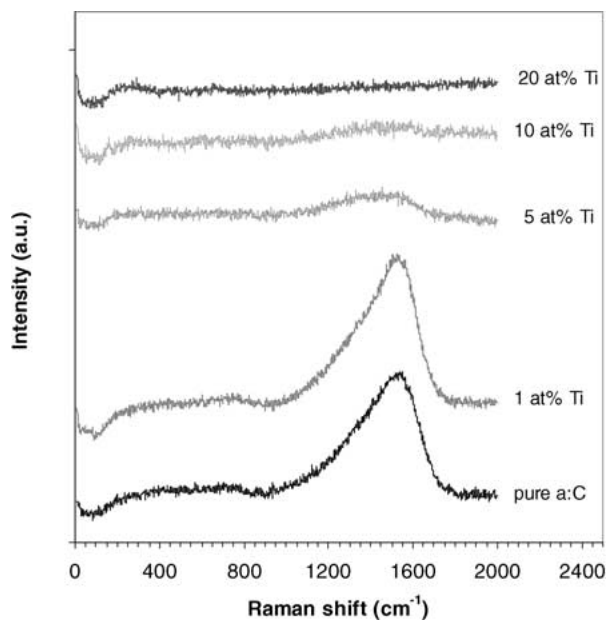
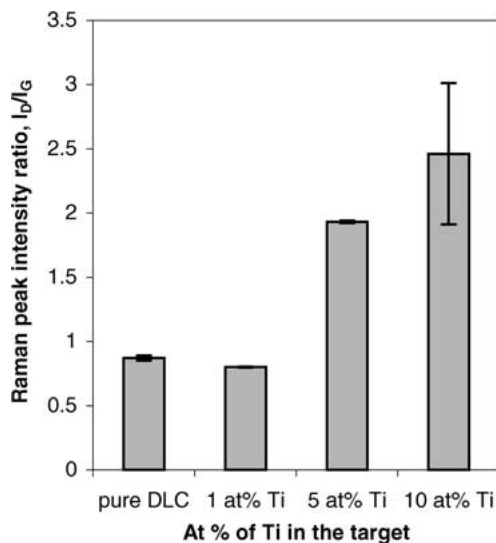


Figure 2 Raman spectra of the pure and Ti-containing a:C films.



(I_D/I_G) and the G-peak width (FWHM) of the films plotted as a function of Ti content in the target is given in Fig. 3. It can be observed from the Figure that the I_D/I_G ratio increases with increasing Ti content in the target. It is reported that the I_D/I_G ratio has some correlation with the sp^3 fraction in the a:C film [15]. Therefore the increase in I_D/I_G ratio with increasing Ti content might imply that the sp^3 content decreases with increasing Ti content in the film. The G-peak width is determined by several factors, and the intrinsic compressive stress is being one of them [16–18]. It can be seen from the Figure that the G-peak width decreases as the Ti content increases. This is probably due to the lowering of the compressive stress present in the film, which is verified in the later part.

3.2. XRD patterns

3.2.1. Crystalline structure of the films

Fig. 4 shows the XRD patterns of the Ti-a:C samples with varied percentage of Ti, acquired with a glancing angle of 0.5° . No obvious crystalline phase can be detected in the films with lower Ti content (1 and 5 at.%).

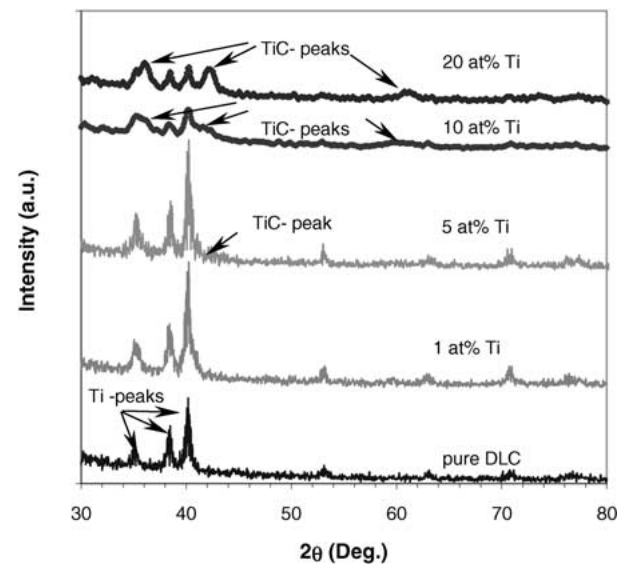


Figure 4 XRD-patterns of a:C films with varied at.% of Ti.

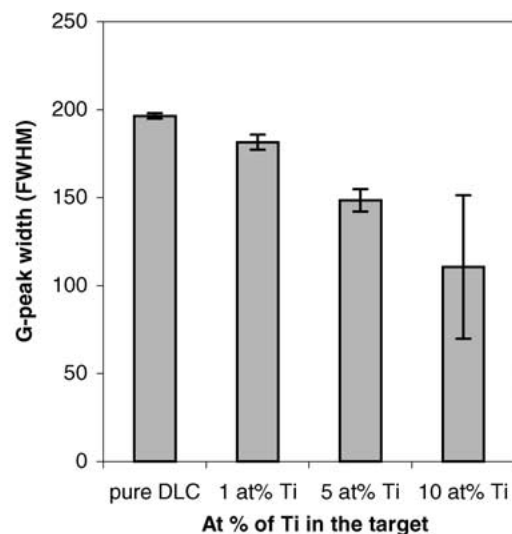


Figure 3 Variation of Raman peak intensity ratio and G-peak width with percentage of Ti in the target.

However in the case of the films prepared with higher at.% of Ti-containing carbon target (10 and 20 at.% Ti), the clear evidence of titanium carbide (TiC) crystalline phase can be observed. This suggests that titanium carbides are formed during the growth and the intensity of it increases with increasing Ti content in the target. Titanium oxides were also found in the film (the XPS data not shown here), and it is difficult to eliminate the oxides trapped in the target during the target compression as well as the native oxides on the Ti particles.

3.2.2. Measurement of film stress using XRD

Stress measurement by radius of curvature method is quite common when the film is prepared on silicon substrates. However this method is not suitable for the measurement of stress, in the case of films that are prepared on metal substrates. The X-ray diffraction is being widely used to measure the residual stress in metals and alloys. Hence, the stress in the Ti-a:C films were determined using XRD. The details of the measurement method are given elsewhere [20]. Since pure a:C, 1 and 5 at.% Ti-a:C did not display strong titanium carbide peaks, the Ti peak at around 114° were chosen for the measurement. The Young's modulus and Poisson's ratio of pure Ti (120.2 GPa and 0.361) are used in the calculation.

Fig. 5 shows the variation of stress with increasing percentage of Ti in the target. It is obvious that the compressive stress in the film decreases with increasing Ti content in the target. This could be due to the reduction in the sp^3 bonded carbon atoms. The result suggest that it is possible to achieve near zero stress amorphous carbon films by preparing it with a 5 at.% Ti-containing carbon target under a substrate pulse bias voltage of 7 kV (300 Hz and 25 μ s). It can also be observed from the Figure that the intrinsic stress becomes tensile when the Ti content in the film is higher.

3.3. Surface morphology

Fig. 6 displays the variation of average roughness of the films as a function of Ti content in the target. Pure a:C film, 1 and 5 at.% Ti-a:C film are observed to be smooth compared to the remaining Ti-a:C films, which

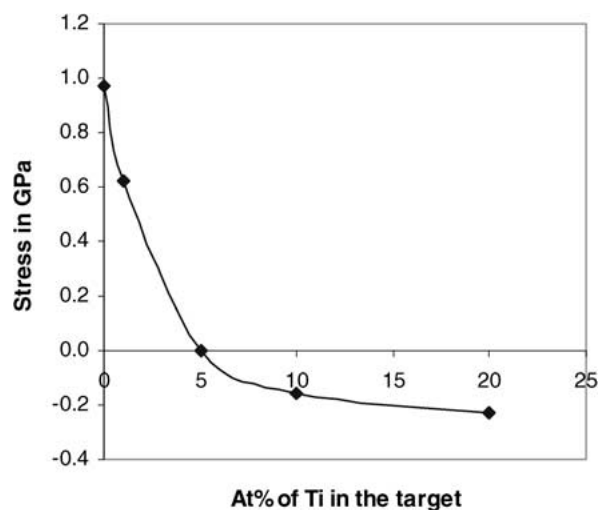


Figure 5 Variation of stress with at.% of Ti in the target.

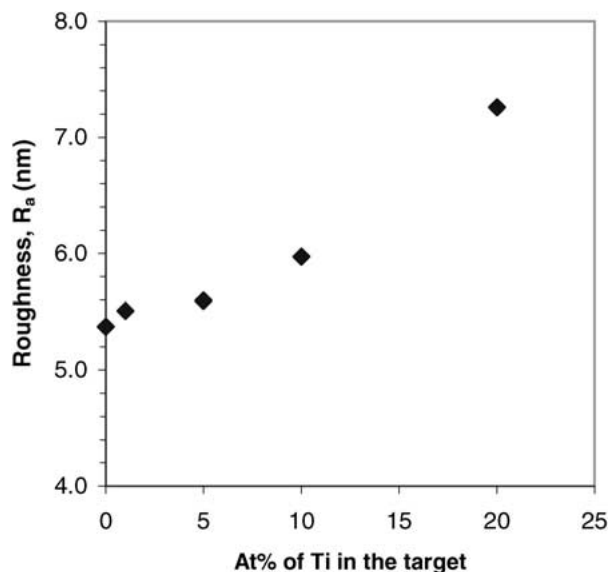


Figure 6 Average surface roughness of the films.

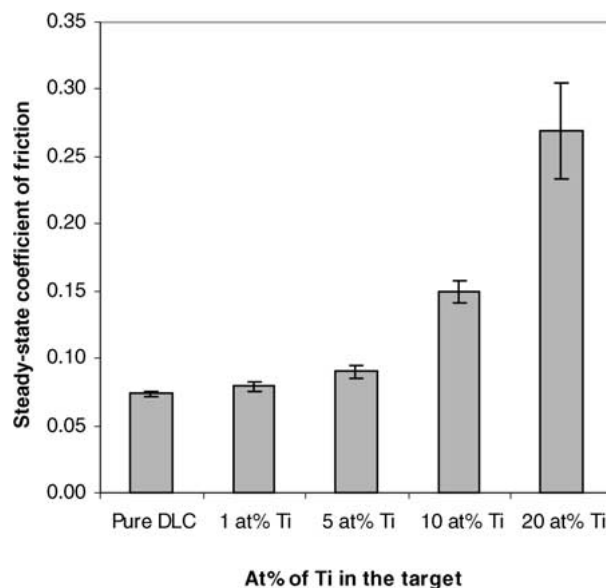


Figure 7 Coefficient of friction of the films.

are prepared with 10 and 20 at.% Ti-containing carbon target. The increasing roughness could be due to the increased amount of metal content in the film.

3.4. Coefficient of friction

The variation of steady state coefficient of friction of the Ti-a:C films as a function of at.% of Ti in the target is given in Fig. 7. The coefficient of friction of pure a:C is around 0.074, and the value increases from 0.079 to 0.269 as the Ti content in the target increases from 1 to 20 at.%. In the case of pure a:C film, graphitisation occurs during sliding and the graphite particles acts as solid lubricant due to their lamellar structure. The increased amount of Ti in the film can reduce the lubricating effect caused by the graphite particles. The tests were carried out at different track radii to verify the results.

3.5. Adhesion

Adhesion of the films in terms of critical load as a function of Ti content in the target is given in Fig. 8. A slight

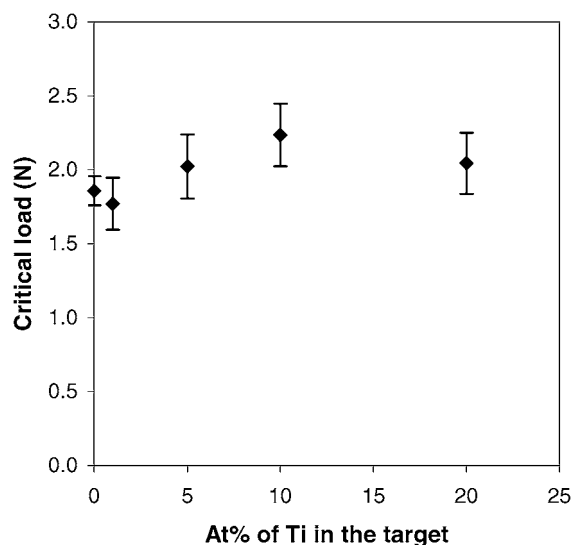


Figure 8 Adhesion of the films in terms of critical load.

increase in critical load can be observed for 1 to 10 at.% Ti-a:C films, however the change is less significant and within the error limit. It was thought that the Ti in the film could bond well with the substrate Ti and hence an improved adhesion with improved Ti content in the film. It has been observed from the previous section that the coefficient of friction increases with increasing Ti content in the film. It is reported that the critical load is inversely proportional to the coefficient of friction [21]. Therefore the increased coefficient of friction of the films might have some bearing on the less significant increase in critical load especially for the film prepared with 20 at.% Ti-containing carbon target.

4. Discussion

The Raman spectra clearly show that the carbon peak intensity decreases with increasing Ti content in the target. The obvious reduction starts only from 5 at.% Ti (target) onwards. This is because the 1 at.% Ti in the target contains only around 1.2 at.% Ti in the film. However the 5, 10 and 20 at.% Ti in the target can obtain about 12.5, 21.4 and 46.0 at.% of Ti in the film [19]. Therefore, the reduction in sp^3 carbon content (increase in I_D/I_G ratio) is expected due to the increase in Ti content in the film. Increase in G-peak width caused by the reduction in compressive stress in the film is verified from the stress measurement using XRD. The XRD patterns also reveal that the Ti bonds with carbon and form of TiC nano-crystallites and it increases with increasing Ti content in the target.

The increase in coefficient of friction with increasing Ti content in the film might be due to the reduction in lubricating ability by the pure graphite particles. Three-body abrasions by the harder titanium carbide (hardness value of 30 GPa) or titanium oxide particles (increases with increasing Ti content) may possibly have a major role in the enhancement of friction.

5. Conclusion

The characterisation of the Ti-containing a:C films with varied percentage of Ti, deposited on pure Ti sub-

strates using FCVA technique suggests that one can prepare films with zero stress by preparing it with 5 at.% Ti-containing carbon target, under 7 kV substrate pulse bias voltage. The morphological surface roughness and coefficient of friction found to increase with increasing Ti content in the film. However, such low stress films may be beneficial for other applications such as thin film passive devices. In conclusion, the film prepared with 5 at.% Ti-containing carbon target produces optimum properties such as almost zero stress, relatively smooth and exhibit low friction compared to that of 20 at.% Ti-a:C film.

References

1. P. J. MARTIN and A. BENDAVID, *Thin Solid Films* **394** (2001) 1.
2. X. SHI, B. K. TAY, D. I. FLYNN and Z. SUN, *Mat. Res. Soc. Symp. Proc., Materials Research Society* **436** (1997) 293.
3. S. ANDERS, D. L. CALLAHAN, G. M. PHARR, T. Y. TSUI and C. S. BHATIA, *Surface and Coating Technology* **94/95** (1997) 189.
4. G. M. PHARR, D. L. CALLAHAN, S. D. MCADAMS, T. Y. TSUI, S. ANDERS, A. ANDERS, J. W. AGER III, I. G. BROWN, C. S. BHATIA, S. R. P. SILVA and J. ROBERTSON, *Appl. Phys. Lett.* **68** (1996) 779.
5. IAN G. BROWN, *Annu. Rev. Mater. Sci.* **28** (1998) 243.
6. T. A. FRIEDMAN, J. P. SULLIVAN, J. A. KNAPP *et al.*, *Appl. Phys. Lett.* **71**(26) (1997) 3820.
7. S. ANDERS, J. DIAZ, J. W. AGER III, R. Y. LO and D. B. BOGY, *ibid.* **71/23** (1997) 3367.
8. O. R. MONTEIRO, J. W. AGER III, D. H. LEE, R. YU LO, K. C. WALTER and M. NASTASI, *J. Appl. Phys.* **88**(5) (2000) 2395.
9. B. K. TAY, Y. H. CHENG, X. Z. DING, S. P. LAU, X. SHI, G. F. YOU, D. SHEEJA, *Diamond and Related Materials* **10**(3-7) (2001) 1082.
10. A. A. VOEVODIN, S. V. PRASAD and J. S. ZABINSKI, *J. Appl. Phys.* **82**(2) (1997) 855.
11. D. SHEEJA, B. K. TAY, S. P. LAU and XU SHI, *Wear* **249** (2001) 433.
12. D. SHEEJA, B. K. TAY, X. SHI, S. P. LAU, C. DANIEL, S. M. KRISHNAN and L. N. NUNG, *Diamond and Related Materials* **10**(3-7) (2001) 1043.
13. SHI XU, B. K. TAY, H. S. TAN, LI ZHONG, Y. Q. TU, S. R. P. SILVA and W. I. MILNE, *J. Appl. Phys.* **79**(9) (1996) 7234.
14. S. PRAWER, K. W. NUGENT, Y. LIFSHITZ, G. D. LEMPERT, E. GROSSMAN, J. KULIK, I. AVIGAL and R. KALISH, *Diamond and related materials* **5** (1996) 433.
15. B. K. TAY, X. SHI, H. S. TAN, H. S. YANG and Z. SUN, *Surface and Coatings Technology* **105** (1998) 155.
16. J. R. SHI, X. SHI, Z. SUN, E. LIU, B. K. TAY and S. P. LAU, *Thin solid films* **366** (2000) 169.
17. M. A TAMOR and W. C VASSELL, *J. Appl. Phys.* **76**(6) (1994) 3823.
18. J. SCHWAN, S. ULRICH, V. BATORI, H. EHRHARDT and S. R. P. SILVA, *ibid.* **80**(1) (1996) 440.
19. X. DING, Y. J. LI, Z. SUN, B. K. TAY, S. P. LAU, G. Y. CHEN, W. Y. CHEUNG and S. P. WONG, *Jl. of Applied Physics* **88**(11) (2000) 6842.
20. B. D. CULLITY and S. R. STOCK, "Elements of X-Ray Diffraction" (Prentice-Hall, Upper Saddle River, New Jersey, 2001).
21. K. HOLMBERG and A. MATTHEWS, "Tribology Series," edited by D. Dowson (Elsevier Science B. V., Amsterdam, 1994) p. 279.

Received 2 May
and accepted 4 September 2002